Experimental Analysis of 10Gb/s Optical OFDM Based on Intensity Modulation with Direct Detection

Abdulamir Ali[1], Jochen Leibrich[1], Henning Paul[2], Annika Dochhan[1], Werner Rosenkranz[1], Karl-Dirk-Kammeyer[2]

[1] Christian-Albrechts-Universität zu Kiel
Kaiserstraße 2
24143 Kiel
aal@tf.uni-kiel.de

[2] Universität Bremen
Otto-Hahn-Allee NW1
28359 Bremen

Abstract

It is the purpose of this contribution to experimentally verify recent theoretical outcomes related to the trade-off between spectral efficiency and receiver sensitivity on one hand and the interplay of modulator biasing and modulator driving voltage swing for optimum receiver sensitivity on the other hand.

1 Introduction

The technology of orthogonal frequency-division multiplexing (OFDM), very well known in classical digital communications, has entered the field of optical communications a few years ago. Following theoretical and numerical analysis, first experimental results on optical OFDM were presented in 2007 using either direct detection [1] or coherent detection [2,3].
Due to the linear relationship between the complex envelope of the optical field and the electrical signal, coherent detection is straightforward in theory but requires some effort in implementation. On the other hand, in case of direct detection the photodiode performs a squaring operation on the optical field resulting in rather challenging theoretical analysis of a fairly simple setup. Some of those aspects, like power fading due to fiber dispersion motivating the implementation of single sideband transmission, meanwhile are known and have already been shown experimentally [1]. Other issues like impact of modulator biasing and driving voltage swing on receiver sensitivity, nonlinear distortions and spectral efficiency [4,5] have been clarified theoretically just recently.

2 Experimental Setup

2.1 Overview

The experimental setup is a hybrid software/hardware setup as shown in **Fig. 1**. The OFDM signal is generated in software on a computer. An arbitrary waveform generator (AWG) serves as high-speed digital-to-analog converter. Both elements are discussed in section 2.2.
The analog signal is transmitted over the optical hardware transmission setup to be described in section 2.3. Using a high-speed real-time sampling oscilloscope, the received signal is converted back into the digital domain, where OFDM demodulation and measurement of the BER are performed off-line (see section 2.4).

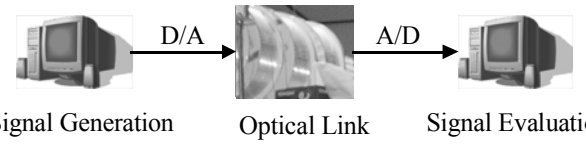

Fig. 1 Hybrid experimental setup (Overview).

2.2 Signal Generation

The block diagram for OFDM signal generation as it is done in software is given in **Fig. 2**. For the digital modulation format, QPSK was selected as it provides a compromise between bandwidth efficiency and sensitivity. To emulate random data with a limited number of complex symbols, for the digital data a pseudo-random quaternary sequence (PRQS) was used [6].

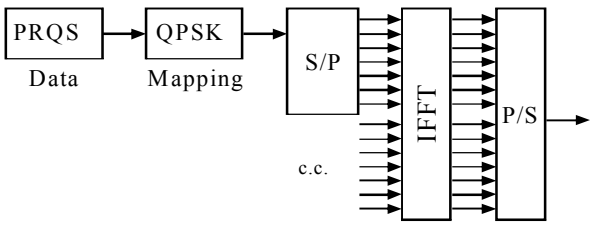

Fig. 2 OFDM signal generation.

The quaternary sequence is mapped onto complex QPSK symbols using grey coding. The serial symbols are parallelized and fed into an IFFT block of size N_{FFT}=1024 for OFDM modulation. For a simple amplitude modulation, avoiding I/Q-modulation, the modulator drive signal must be real. To generate a real-valued IFFT output, the total IFFT input is composed of the complex data and its complex conjugate. To be precise, for an IFFT of length N_{FFT}=1024, 511 inputs are filled with data, 511 inputs are generated using conjugate complex operation, finally the

two inputs at DC and half sampling frequency need to be set to zero. The IFFT output is serialized to generate the OFDM signal in time domain.

According to specification, the AWG provides an output bandwidth of 5.8 GHz and a sampling frequency of 20 Gsamples/s. Measurements confirmed a 3dB bandwidth of around 5-6 GHz. For QPSK modulation, using 5 GHz signal bandwidth the maximum data rate is nearly 10Gb/s if all 511 subcarriers are filled with data. However, in order to increase robustness towards nonlinearity of Mach-Zehnder modulator (MZM) and photodiode, a well known approach is to allocate only the upper half of the subcarriers (i.e. 256 subcarriers for N_{FFT}=1024). This generates sufficient space in frequency domain to capture signal contributions due to quadratic nonlinearity [7], but at the same time it reduces the data rate to 5Gb/s. However, independent of the subcarrier allocation, for the evaluation of the BER each time 1024 OFDM symbols are transmitted at a symbol rate of ≈9.75 MBaud.

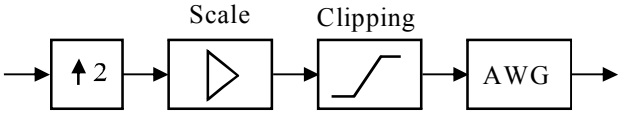

Fig. 3 Preparation of OFDM signal for driving the AWG.

The OFDM signal at the output of the serializer in Fig. 2 is sampled at a frequency of 10 Gsamples/s. To adapt to the sampling frequency required for the AWG, according to **Fig. 3** the signal is upsampled to 20 Gsamples/s. Before the signal is transferred to the AWG via LAN connection, it is scaled and clipped appropriately to achieve the amplitude range required for the AWG. Details on clipping and scaling (i.e. amplification) are discussed in the next subsection.

2.3 Hardware Setup

The AWG provides the interface between software and hardware implementation on transmitter side. The hardware part of the transmitter is given in **Fig. 4**. A critical issue is generation of the driving voltage of the MZM. The AWG provides output peak-to-peak voltage of 0.5 V. The switching voltage of the MZM was measured to be equal to V_π=8 V.

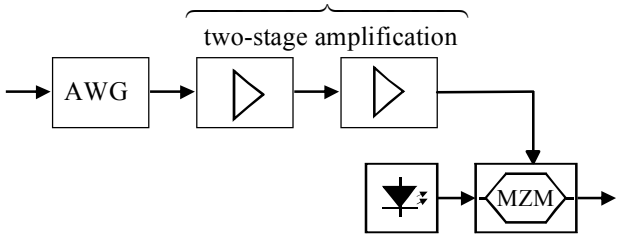

Fig. 4 Transmitter setup.

To be able to make use of the full transfer characteristic of the MZM (see **Fig. 5**), amplification of 24 dB is required which requires two-stage amplification. As multicarrier signals are very sensitive to nonlinearity, care needs to be taken to drive the second amplifier in the linear regime by insertion of appropriate attenuation between both amplifiers (G_1=17 dB, G_2=19 dB).

The modulation format for transmission of the quasi-analog OFDM-signal is simple amplitude modulation with carrier. Carrier power is set by means of the bias voltage V_{bias} added to the driving signal $s(t)$. The input-output power characteristic is shown in Fig. 5.

The achievable receiver sensitivity depends on modulation depth and can be improved by optimizing the MZM bias point [8]. The modulation depth is tuned in software by means of proper scaling (see Fig. 3). It is measured as standard deviation normalized by the switching voltage, i.e. as σ_s/V_π.

To avoid overdriving the MZM, clipping is performed to limit the peak-to-peak voltage to V_π. The actual clipping thresholds need to be adapted to the bias point. If the MZM is operated e.g. at quadrature point (V_{bias}=0.5V_π), the clipping limits are symmetrical at ±V_π/2. For different values of the bias, non-symmetrical clipping is performed (e.g. +0.3V_π to -0.7V_π for V_{bias}=0.7V_π).

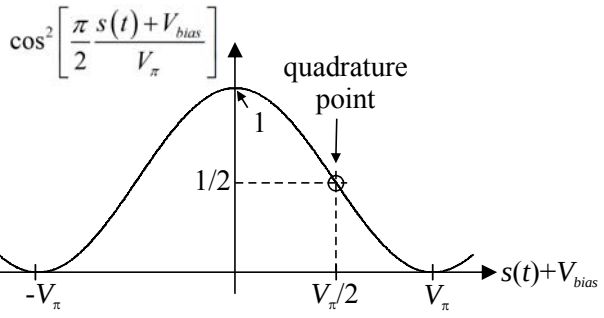

Fig. 5 Power transfer characteristic of MZM.

After transmission over the optical transmission line, the signal is fed into an attenuator followed by an optical pre-amplifier for ASE-noise loading. The OSNR is measured with an optical spectrum analyzer and the signal is detected by a photo receiver with electrical bandwidth B_e=12 GHz. The received signal sent to the input of the real-time sampling oscilloscope.

2.4 Signal Evaluation

The real-time sampling oscilloscope is the interface between hardware implementation and software signal evaluation as depicted in **Fig. 6**. The sampling rate of the real-time oscilloscope is equal to 50 Gsamples/s. The time duration of 1024 OFDM symbols at a rate of ≈9.75 MBaud is equal to ≈105µs. This results in at least 5.25 million samples to record by the oscilloscope.

In order to be able to compare the received signal and the reference signal that was sent into the AWG (i.e. the transmitted signal), the incoming signal is downsampled by a factor of 2.5. Although the sample clocks of AWG and oscilloscope were not explicitly synchronized, sufficient stability was observed during recording time such that additional effort for synchronization is not required.

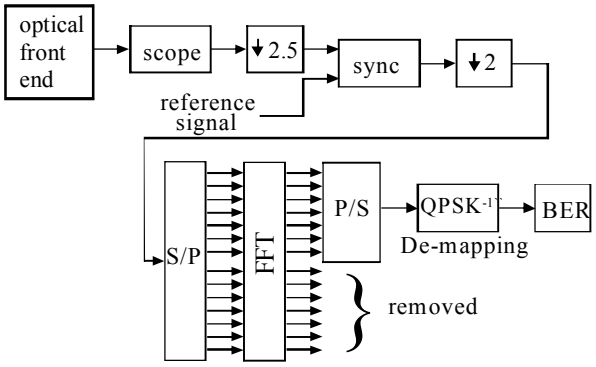

Fig. 6 Signal synchronization, OFDM demodulation and BER measurement.

For OFDM symbol synchronization, 4 symbols of the reference signal are correlated with the whole downsampled data signal. The synchronization process is carried out in two stages. First, the sampled signals are correlated directly. Having found the maximum, time synchronization is performed on sub-sample scale by finding the linear phase in frequency domain that is required for maximization of correlation.

After further downsampling by another factor of two, the OFDM signal is obtained with a sampling frequency of 10 GHz. OFDM demodulation is carried out in reverse order compared to OFDM modulation. Finally, the BER is measured. In case of 10 Gb/s, 2^{19}=Bit are obtained per I- and Q-contribution. In case of 5 Gb/s the number is reduced to 2^{18}. Since a significant difference in BER between I- and Q-contributions was not observed, the final BER is obtained by taking the mean.

3 Degrading Impairments

3.1 ASE-Noise

In section 4, the BER is measured as function of the optical signal-to-noise ratio (OSNR), which makes sense as noise generated by the optical preamplifier plays a central role in any optically amplified transmission system.

Assuming low modulation depth, in [9] an analytical expression for the BER as a function of OSNR in QPSK-modulated direct detection optical-OFDM transmission is derived:

$$BER = \frac{1}{2}\operatorname{erfc}\left(\sqrt{\frac{\pi^2}{4}\cdot\frac{B_o'}{B_e}\cdot\left(\frac{\sigma_s}{V_\pi}\right)^2\cdot\tan^2\left(\frac{\pi}{2}\frac{V_{bias}}{V_\pi}\right)\cdot OSNR}\right) \quad (1)$$

Here, 'erfc' denotes the complementary error function, B_e is the received electrical bandwidth and the OSNR is measured within B_o'=12.5 GHz, which is equivalent to 0.1nm in the 1550nm wavelength range.

3.2 Other impairments

Besides ASE-noise, MZM nonlinearity, photodiode nonlinearity (second order intermodulation distortion IMD), linear distortion and thermal noise play important roles for achievable receiver sensitivity. As the power budget of the driving amplifiers was designed carefully, the main origin of nonlinearity in a back-to-back scenario can be found in the MZM characteristic.

As the transmission channel can be considered as ideal in the back-to-back case, now significant linear distortion is expected. Nevertheless, the limited output bandwidth of the AWG results in slight attenuation of the higher subcarriers. In future work, equalization of this transfer function is aimed at, but in the current state compensation is not realized. Therefore, reduction of bandwidth of the photo receiver of 12 GHz to suppress thermal noise by subsequent filtering is not carried out to avoid increase of linear distortion. This leaves room for further optimization of the receiver.

4 Results and Discussion

4.1 Overview

As depicted in section 3.1, there is a theoretical sensitivity in terms of BER for direct detection optical-OFDM that could be achieved if ASE-noise was the only impairment. However, as also other impairments enumerated in section 3 are present, this theoretical sensitivity cannot be achieved. Instead, a penalty is obtained which depends on the number and the strength of additional impairments.

Especially, the impact of nonlinearity depends on whether all subcarriers are used for data transmission resulting in 10 Gb/s data rate or if the frequency gap is introduced to spectrally separate data and second order nonlinear terms resulting in 5 Gb/s data rate. These two scenarios are considered separately in the following subsections.

4.2 10Gb/s Full Bandwidth

To avoid nonlinearity, in a first step the system is driven with a very small signal with σ_s=0.05V_π. The MZM is biased at quadrature point. Then, the impact of nonlinearity is expected to be negligible allowing for identification of the impact of linear distortion and thermal noise.

According to **Fig. 7**, as can be expected the measured sensitivity is low (e.g. 32 dB OSNR @ BER=10^{-3}). However, the deviation of the measurement result from the theoretical ASE noise limit in the low OSNR range is less than 3dB. Due to low modulation depth, the signal is very sensitive to thermal noise produced in the photo receiver. Thus, the joint impact of IMD, thermal noise and linear distortion adds up to 2.8 dB @ BER=10^{-2}. For higher OSNR, the impact of thermal noise increases and the measurement result deviates more from the ASE noise limit. A BER floor is found at BER≈10^{-5}.

In the next step, several values for the modulation depth are compared. The results are found in **Fig. 8**. First, the modulation depth is doubled to σ_s=0.1V_π. According to (1), theoretically an improvement of 6dB is expected. However, the measured improvement is less, e.g. 4.1 dB @ BER=10^{-2}. This can be interpreted as follows:

On one hand, for σ_s=0.1V_π signal degradation due to MZM nonlinearity is obtained reducing the improvement to ≈3.5dB (see Fig. 7). On the other hand, higher modulation depth results in higher robustness towards thermal noise. Therefore, a BER floor is found at BER≈10^{-6}. for σ_s=0.15V_π, improvement of only less than 2dB over σ_s=0.1V_π is achieved because of MZM nonlinearity and also a BER floor is found at BER≈10^{-6}. for σ_s=0.2V_π, the MZM nonlinearity will be higher and therefore a BER floor is found at BER≈10^{-4}.

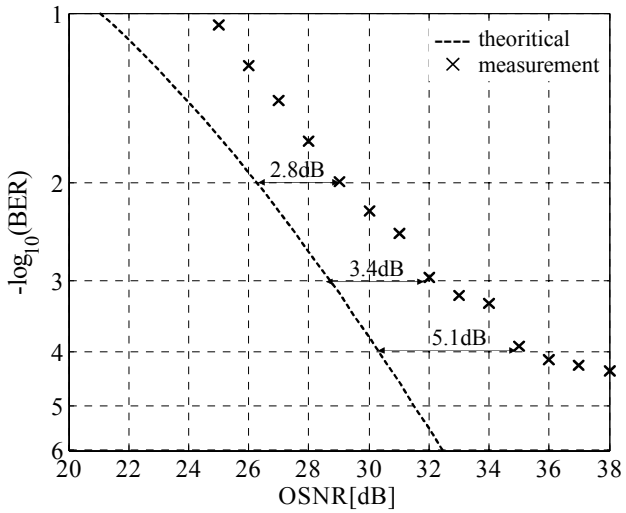

Fig. 7 Comparison of theoretical result and measurement result for σ_s=0.05V_π and biasing at quadrature point.

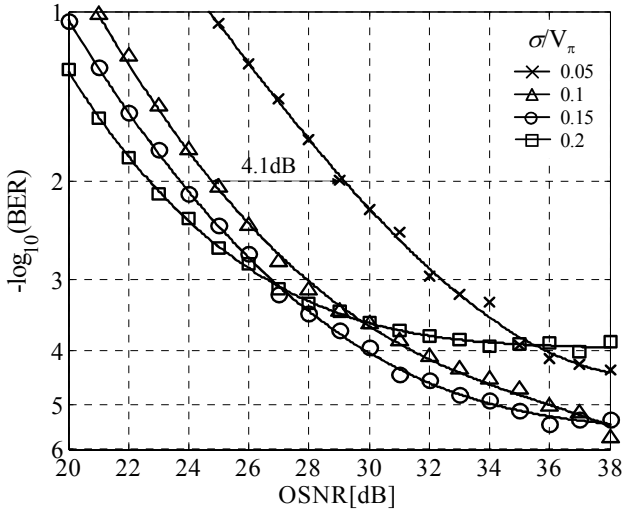

Fig. 8 Sensitivity depending on modulation depth for biasing at quadrature point.

The fact that significant nonlinearity is obtained is supported by the results for σ_s=0.2V_π. For low OSNR, an improvement of significantly less than further 6dB is obtained. For increased OSNR, however, the limiting impact of nonlinearity starts rapidly resulting in a floor at BER≈10^{-4}.

From the result in Fig.8, we can see that a BER floor is occurring for small and large driving signals. This can be attributed to the IMD from PD which causes an inband distortion. Thus in the next, the signal band is displaced from the optical carrier by a frequency gap (W_g) which ensures that the second-order intermodulation distortion (IMD), due to photodetection, will mainly fall outside the OFDM band

4.3 5Gb/s Half Bandwidth

To introduce frequency gap, the first half of the subcarriers is set to zero. A comparison of receiver sensitivity between the previous system (without frequency gap) and the current system (with frequency gap) is performed for the same driving signal σ_s=0.05V_π and same biasing point (quadrature) as depicted in **Fig. 9**.

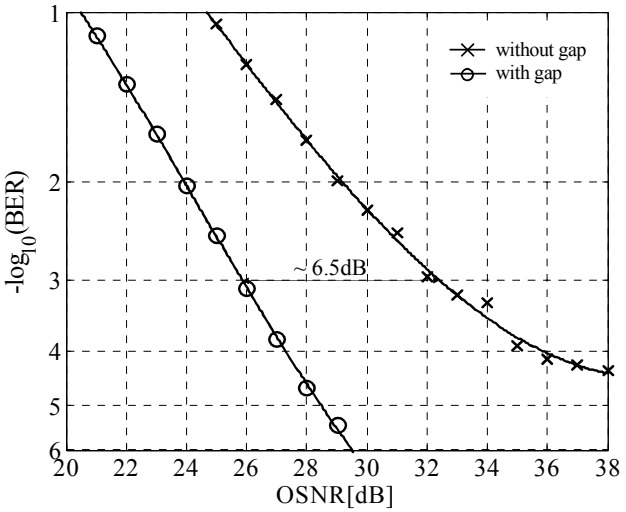

Fig. 9 Advantage of frequency gap for σ_s=0.05V_π and biasing at quadrature point.

From Fig. 9, an improvement of ≈6.5dB is achieved at BER=10^{-3}. The first 3dB for halving the data rate and the other 3.5 dB is after adding the frequency gap. In addition, no BER floor is occurs, which means that the system is robust towards thermal noise even for a small driving signal. Again, several values for the modulation depth are compared. The results are found in **Fig. 10**. As we can see, a sensitivity improvement is achieved for all modulation depths. BER floor is observed only for σ_s=0.2V_π at BER≈10^{-5} (compare with Fig. 8).

The previous results show the basic dilemma when the MZM is biased at the point of highest linearity. To avoid nonlinear distortion the driving amplitude still has to be chosen sufficiently low. The power of the optical carrier wastes a high percentage of the total power. Therefore, in the following a variable bias is introduced.

Fig. 11 shows the results for different values of bias and σ_s=0.05V_π. Choosing the bias voltage such that carrier power is reduced (i.e. on the power characteristic given in Fig. 5 we move to the right) improves sensitivity, but at the cost of worse linearity. As long as the resulting degradation does not over compensate for the benefit due to reduced carrier power, receiver sensitivity increases.

Further sensitivity improvement has been achieved with variable bias values after increasing the amplitude of the driving signal to σ_s=0.2V_π as shown in **Fig. 12**.

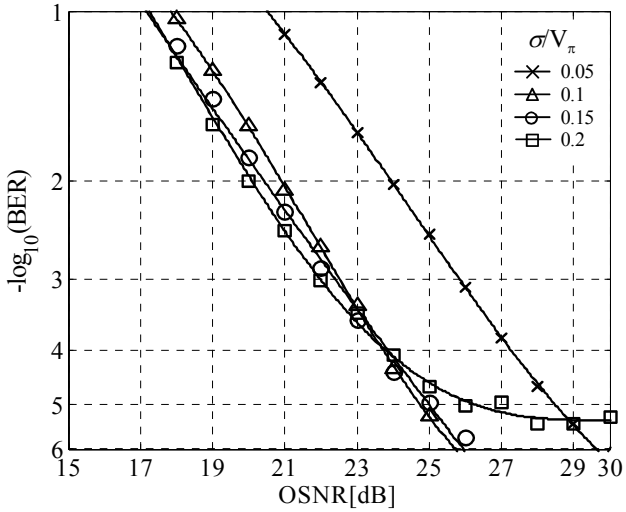

Fig. 10 Sensitivity depending on modulation depth for biasing at quadrature point.

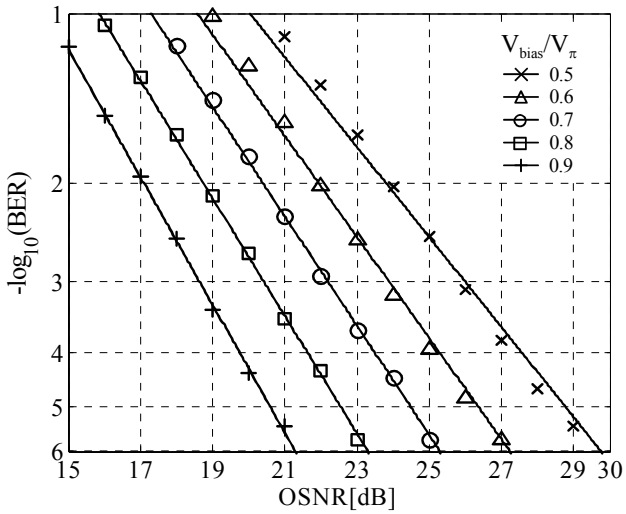

Fig. 11 Sensitivity depending on biasing point for $\sigma_s=0.05V_\pi$.

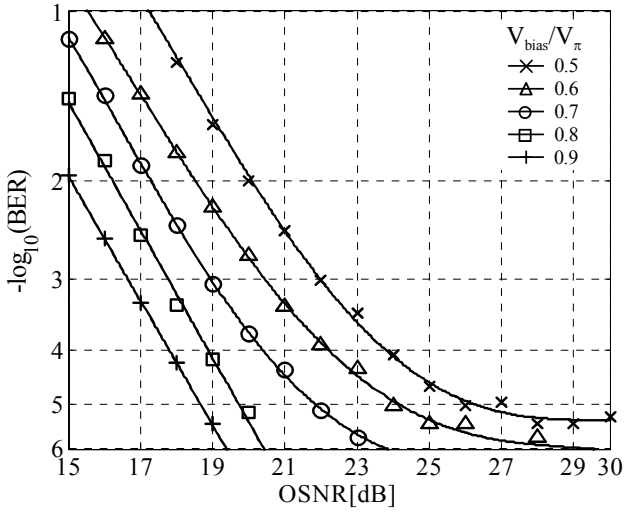

Fig. 12 Sensitivity depending on biasing point for $\sigma_s=0.2V_\pi$.

For $V_{bias}=0.5V_\pi$, the signal is clipped symmetrically and the BER floor is found at BER$\approx 10^{-5}$. After increasing the bias value the OFDM signal exhibits an asymmetrical clipping and the BER floor goes to zero, which means that an asymmetrical clipping of an OFDM signal results in better performance than symmetrical clipping.

5 Conclusions

In an experimental assessment we have investigated the influence of the frequency gap, signal amplitude and the biasing point on the receiver sensitivity for direct detection optical-OFDM system with back-to-back transmission. Adding a frequency gap improves the sensitivity but on the other hand reduces the spectral efficiency. Proper selection of signal amplitude and modulator bias improves the sensitivity by several dB.

Further improvement can be achieved by using optical filter for ASE noise reduction and filtering after the photodiode to reduce the thermal noise.

6 References

[1] B.J.C. Schmidt, A.J. Lowery, and J. Armstrong, "Experimental demonstrations of 20 Gbit/s direct-detection optical OFDM and 12 Gbit/s with a colorless transmitter," *OFC 2007*, paper PDP18.

[2] S. L. Jansen, I. Morita, N. Takeda, H. Tanaka, "20-Gb/s OFDM transmission over 4,160-km SSMF enabled by RF-pilot tone phase noise compensation," *OFC 2007*, paper PDP15.

[3] Y. Ma, W. Shieh and X. Yi " Characterisation of nonlinearity performance for coherent optical OFDM signals under influence of PMD," Electronics Letterers, Vol. 43, No. 17, 2007.

[4] J. Leibrich, A. Ali, and W. Rosenkranz, "OFDM transceiver design for optimizing sensitivity and long-haul performance," *IEEE LEOS Summer Topicals 2008*, paper WD3.1.

[5] A. Ali, J. Leibrich, and W. Rosenkranz, "Spectral efficiency and receiver sensitivity in direct detection optical-OFDM," *OFC 2009*, paper OMT7.

[6] B. Spinnler and C. Xie "Performance Assessment of DQPSK using Pseudo-Random Quaternary," *ECOC 2007*.

[7] A. J. Lowery and J. Armstrong,"Orthogonal-frequency-division multiplexing for optical dispersion compensation," in *OFC 2007*, Anaheim, California, USA, Paper OTuA4.

[8] J. Leibrich, A. Ali and W. Rosenkranz, "OFDM Transceiver Design for Optimizing Sensitivity and Long-Haul Performance," invited to LEOS Summer Topic on Next Generation Transceiver Tech. for Long Haul Optical Comm., 2008.

[9] J. Leibrich, A. Ali, H. Paul, W. Rosenkranz and K.D. Kammeyer "On the Impact of Biasing for Direct Detection OFDM," submitted to Photonic Technology Letter.